

The “Resonances Via Padé” (RVP) Method

Ralf-Arno Tripolt, ECT*, Trento, Italy

Based on arXiv: 1610.03252

Ralf-Arno Tripolt, Idan Haritan, Jochen Wambach, Nimrod Moiseyev

LNF, Frascati, February 28th, 2017

ECT*

EUROPEAN CENTRE FOR THEORETICAL STUDIES
IN NUCLEAR PHYSICS AND RELATED AREAS

Outline

I) “Resonances Via Padé” (RVP) Method

- ▶ Definition and Properties

II) Applications

- ▶ simple examples
- ▶ extraction of complex resonance poles and decay thresholds
- ▶ analytic continuation - from imaginary to real time

III) Summary

I) “Resonances Via Padé” (RVP) Method

$$\begin{aligned} S_p[\psi, \bar{\psi}, A] &= \sum_{n=0}^{\infty} \int d^6x \times \bar{\psi}^{(n)} \left[\psi_{\mu} \partial_{\nu} + i g \left(\partial_{\mu} \psi \right) - m \right] \psi^{(n)} \rightarrow S_0[A] = \sum_{n=0}^{\infty} \int d^6x F_{\mu\nu} \psi_{\mu} \bar{\psi}_{\nu} \psi^{(n)} \\ \psi(x) \rightarrow \psi'(x) &= \Omega(x) \psi(x) \wedge \bar{\psi}(x) \rightarrow \bar{\psi}'(x) = \bar{\psi} \Omega^{\dagger}(x) \rightarrow S_0[\psi, \bar{\psi}, A] = S_0[\psi', \bar{\psi}', A] \cdot S_0[m, \bar{m}] \cdot S_0[m, \bar{m}] \\ \Omega^{\dagger} \left[\partial_{\mu} \left(\Omega \partial_{\mu} \psi \right) \right] &= \Omega^{\dagger} \left[\left(\partial_{\mu} \Omega \right) \psi + \Omega \left(\partial_{\mu} \psi \right) \right] = \left[\partial_{\mu} \Omega + \Omega^{\dagger} \Omega \partial_{\mu} \right] \psi = [\Omega^{\dagger} \partial_{\mu} \Omega + \partial_{\mu} \bar{\Omega}] \psi \\ \bar{\psi} \Omega^{\dagger} \left(\partial_{\mu} + i g A_{\mu} \right) \Omega \psi &= \bar{\psi} \left(\partial_{\mu} + i g A_{\mu} \right) \psi \Leftrightarrow \Omega^{\dagger} \left[\partial_{\mu} (\Omega \psi) + i g A_{\mu} (\Omega \psi) \right] = \partial_{\mu} \psi + i g A_{\mu} \psi \\ \Rightarrow S_0'(\Omega, \bar{\Omega}) \psi + i g A_{\mu} \psi &\Leftrightarrow [\Omega^{\dagger} g A_{\mu} \Omega] \psi = \bar{\Omega} \psi + i g \bar{A}_{\mu} \Omega \psi \cdot D_{\mu} = \bar{\Omega} \psi + i g \bar{A}_{\mu} \Omega \psi \\ \Rightarrow A_{\mu} \rightarrow A_{\mu}'(x) &= \Omega(x) A_{\mu}(x) \cdot D_{\mu} = \Omega^{\dagger}(\mu \omega(x)) \Omega(x) \cdot S_0[\psi, \bar{\psi}, A] \cdot S_0[m, \bar{m}] = S_0[\psi', \bar{\psi}', A] \cdot D_{\mu} = \bar{\Omega} \psi + i g \bar{A}_{\mu} \Omega \psi \\ D_{\mu} \rightarrow D_{\mu}''(x) &= \bar{\Omega} \psi + i g \bar{A}_{\mu} \Omega \psi = \bar{\Omega} \psi + i g \bar{A}_{\mu} \Omega \psi = \bar{\Omega} \psi + i g \bar{A}_{\mu} \Omega \psi = \bar{\Omega} \psi + i g \bar{A}_{\mu} \Omega \psi = \bar{\Omega} \psi + i g \bar{A}_{\mu} \Omega \psi \\ F_{\mu\nu} \rightarrow F_{\mu\nu}'(x) &= S_0[\psi, \bar{\psi}, A] \cdot F_{\mu\nu} \psi \\ U_p(\omega) \rightarrow U_{p'}(\omega) &= S_0[\psi, \bar{\psi}, A] \end{aligned}$$


[courtesy L. Holicki]

RVP Method - Definition

Given a finite set of $N = M + 1$ real data points (η_i, F_i) , the aim is to find a function $F(\eta)$ which represents the correct analytic continuation,

$$F(\eta) = \frac{P(\eta)}{Q(\eta)},$$

where $P(\eta)$ and $Q(\eta)$ are polynomials. We construct an approximation to $F(\eta)$ by using the Schlessinger point method

$$C_M(\eta) = \frac{F_1}{1 + \frac{z_1(\eta - \eta_1)}{1 + \frac{z_2(\eta - \eta_2)}{\vdots z_M(\eta - \eta_M)}}},$$

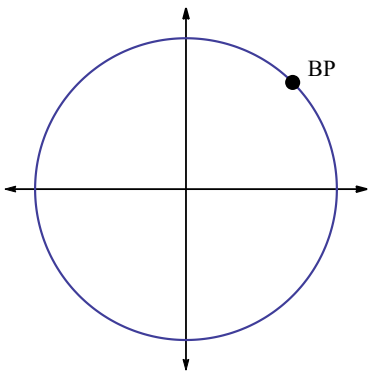
where the z_i are real coefficients chosen such that

$$C_M(\eta_i) = F_i, \quad i = 1, 2, \dots, N.$$

An analytic continuation into the complex plane is performed by choosing η to be complex, i.e. $\eta = \alpha e^{i\theta}$.

RVP Method - Radius of Convergence

- ▶ The radius of convergence of $C_M(\eta)$ is given by the location of the nearest branch point in the complex plane
- ▶ the input points have to be chosen suitably, i.e. from the same analytic regime
- ▶ due to numerical uncertainties and the finite number of input points, $C_M(\eta)$ can also give meaningful results beyond the BPs



II) Applications

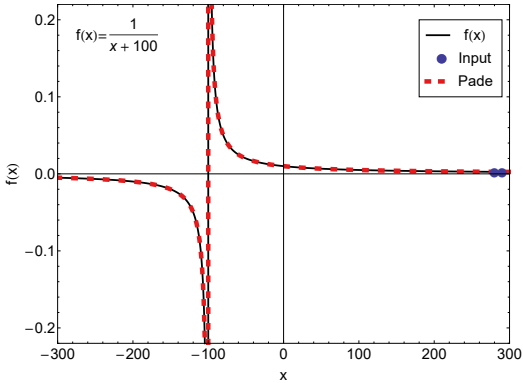
$S_p[\psi, \bar{\psi}, A] = \sum \int d^6x \times \bar{\psi}^{(1)} \left[\gamma_5 (\partial_\mu + i g (\partial_\mu)^{(1)} + m^{(1)}) - \bar{\psi}^{(1)} \right] \rightarrow S[\psi] = \sum \int d^6x T[\bar{\psi}_\mu \psi^{(1)}]$
 $\psi(x) \mapsto \psi'(x) = D(x)\psi(x) \wedge \bar{\psi}(x) \mapsto \bar{\psi}'(x) = \bar{\psi}(x)D^\dagger(x) \rightarrow S[\psi, \bar{\psi}, A] = S[\psi', \bar{\psi}', A'] \cdot S[ms^2 \delta = m]$
 $D^\dagger [\partial_\mu (\Sigma \psi)] = \Sigma^\dagger [(\partial_\mu \Sigma) \psi + \Sigma (\partial_\mu \psi)] = [\partial_\mu \Sigma + \Sigma^\dagger \Sigma \partial_\mu] \psi = [\partial_\mu \Sigma + \Sigma^\dagger \partial_\mu] \psi$
 $\bar{\psi} D^\dagger (\partial_\mu + i g A_\mu) \Sigma \psi = \bar{\psi} (\partial_\mu + i g A_\mu) \psi \Leftrightarrow \Sigma^\dagger [\partial_\mu (\Sigma \psi) + i g A_\mu (\Sigma \psi)] = \partial_\mu \psi + i g A_\mu \psi$
 $\Rightarrow \Sigma^\dagger (\partial_\mu \psi) + i g A_\mu \psi \Leftrightarrow [\Sigma^\dagger g A_\mu \Sigma] \psi = \partial_\mu \psi + i g A_\mu \psi \quad D_\mu = \partial_\mu - g A_\mu$
 $\Rightarrow A_\mu \rightarrow A'_\mu = D(x)A_\mu$
 $D_\mu \rightarrow D'_{\mu\nu} = \partial_\mu + i g A_\mu \delta_{\mu\nu}$
 $F_{\mu\nu} \rightarrow F'_{\mu\nu} = S(x) F_{\mu\nu}$
 $U_\mu(x) \rightarrow U_\mu(x) = 1$



[courtesy L. Holicki]

Simple Examples: $f(x) = 1/(x + 100)$

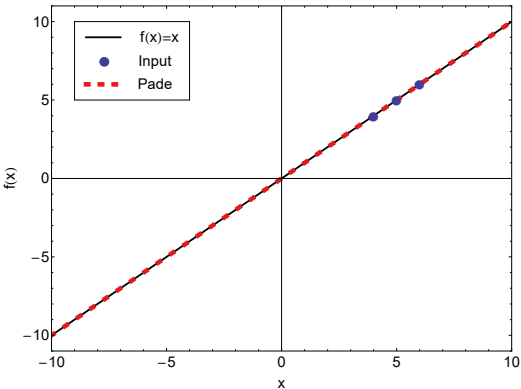
- ▶ Only 2 input points are needed to reconstruct
- $$f(x) = \frac{1}{x+100}$$
- ▶ it is the “first guess” of the method



Simple Examples: $f(x) = x$

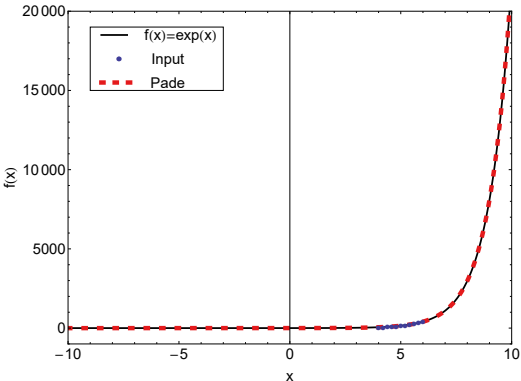
- ▶ 3 input points are needed to reconstruct $f(x) = x$
- ▶ one obtains for example

$$C_M(x) = \frac{22 + 1.8 \cdot 10^{15}x}{1.8 \cdot 10^{15} - x} \approx x$$



Simple Examples: $f(x) = e^x$

- ▶ $N \gtrsim 10$ input points are needed to obtain a reasonable reconstruction of $f(x) = \exp(x)$

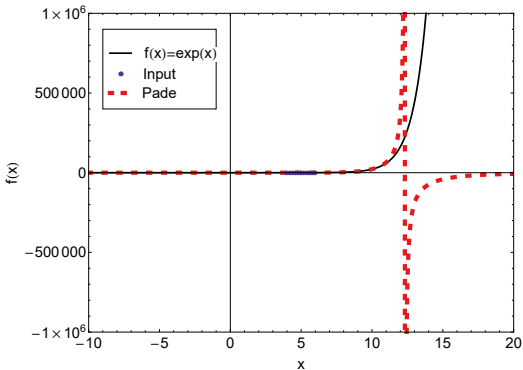


- ▶ for $N = 11$ one obtains for example

$$C_M(x) = \frac{263504 + 170536x + 46451x^2 + 10389x^3 + 756x^4 + 148x^5}{265568 - 98809x + 15473x^2 - 1274x^3 + 55x^4 - x^5}$$

Simple Examples: $f(x) = e^x$

- ▶ $N \gtrsim 10$ input points are needed to obtain a reasonable reconstruction of $f(x) = \exp(x)$

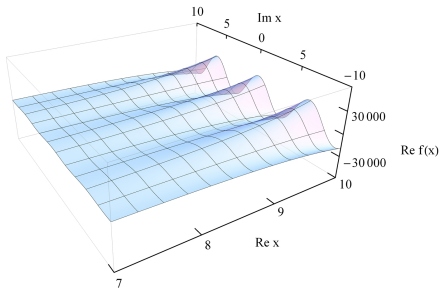


- ▶ for $N = 11$ one obtains for example

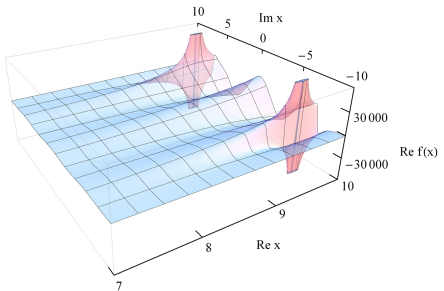
$$C_M(x) = \frac{263504 + 170536x + 46451x^2 + 10389x^3 + 756x^4 + 148x^5}{265568 - 98809x + 15473x^2 - 1274x^3 + 55x^4 - x^5}$$

Simple Examples: $f(x) = e^x$

$\operatorname{Re} \exp(x)$:



$\operatorname{Re} C_M(x)$:



Analytic example for a spectral function (I)

We use

$$\rho(\omega^2) = -\frac{1}{\pi} \text{Im} \left(\frac{1}{\omega^2 - M^2 - \Pi(\omega^2)} \right)$$

with the self energy

$$\Pi(\omega^2) = S_1 \log(T_1^2 - \omega^2) + S_2 \log(T_2^2 - \omega^2)$$

and the parameters

$$M = 50 \text{ MeV},$$

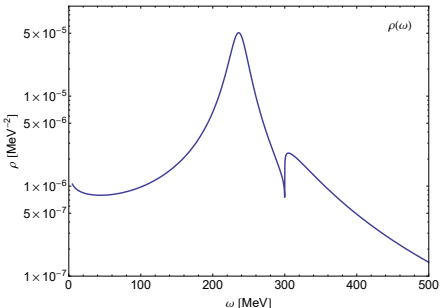
$$S_1 = 2000 \text{ MeV},$$

$$T_1 = 0 \text{ MeV},$$

$$S_2 = 3000 \text{ MeV},$$

$$T_2 = 300 \text{ MeV},$$

$$\omega \rightarrow \omega + i\varepsilon \text{ with } \varepsilon \rightarrow 0$$

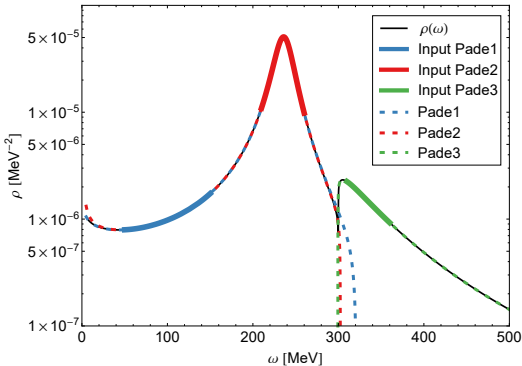


Analytic example for a spectral function (II)

The decay thresholds at $T_1 = 0$ MeV and $T_2 = 300$ MeV represent branch points on the real axis.

Pade1 and Pade2 can be used to study the regime $T_1 < \omega < T_2$, Pade3 for $\omega > T_2$.

$N \approx 50$ input points were used for each regime.



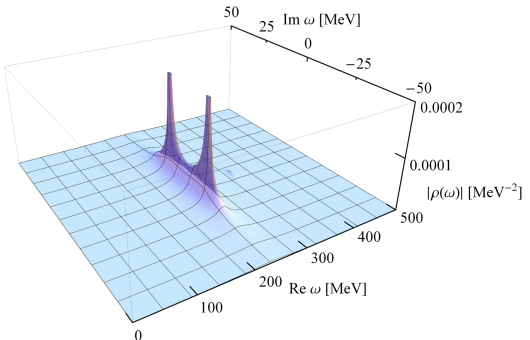
[R.-A. T., I. Haritan, J. Wambach and N. Moiseyev, arXiv:1610.03252]

Analytic example for a spectral function (III)

The complex conjugate poles can be located by using Pade1 or Pade2:

$$\omega_P \approx (236.43 \pm i12.64) \text{ MeV}$$

The intrinsic error of the RVP method is usually negligible and here smaller than 0.01 MeV.



Model for overlapping resonances (I)

We use the Kühn-Santamaria (KS) parametrization for the form factor

$$F(s) = \sum_{i=1}^3 \frac{M_i^2}{M_i^2 - s - i\Gamma_i \frac{M_i^2}{\sqrt{s}} \left(\frac{k(s)}{k(M_i^2)} \right)^3}$$

with

$$k(s) = \frac{\sqrt{s}}{2} \sqrt{1 - 4m_\pi^2/s}$$

and the parameters

$$M_1 = 0.5 \text{ GeV},$$

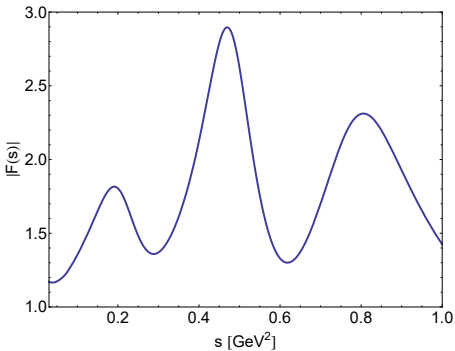
$$\Gamma_1 = 0.2 \text{ GeV},$$

$$M_2 = 0.7 \text{ GeV},$$

$$\Gamma_2 = 0.1 \text{ GeV},$$

$$M_3 = 0.9 \text{ GeV},$$

$$\Gamma_3 = 0.15 \text{ GeV},$$

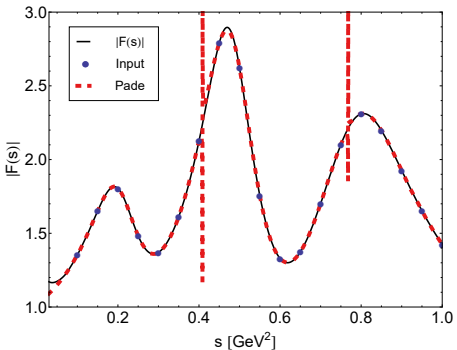


Model for overlapping resonances (II)

$N = 19$ input points were used.

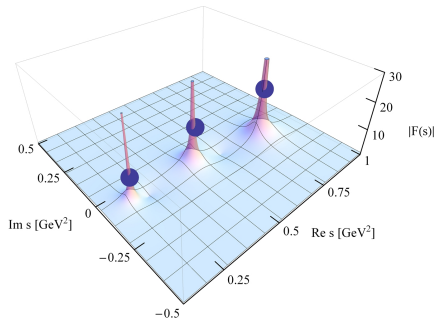
All resonance poles can be reconstructed at the same time since they are in the same analytic regime.

Additional poles can appear in the reconstruction, but they can be easily identified as being unphysical by varying the number of input points or the input region.

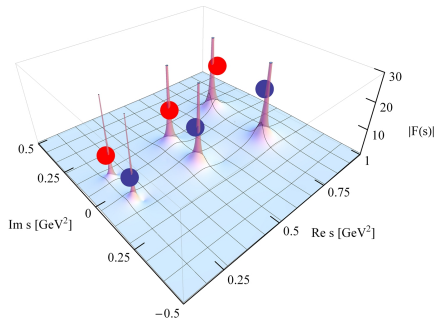


Model for overlapping resonances (III)

exact result, $F(s)$:



reconstruction, $C_M(s)$:



Model for strongly overlapping resonances (I)

We use the KS parametrization for the form factor

$$F(s) = \sum_{i=1}^3 \frac{M_i^2}{M_i^2 - s - i\Gamma_i \frac{M_i^2}{\sqrt{s}} \left(\frac{k(s)}{k(M_i^2)} \right)^3}$$

with

$$k(s) = \frac{\sqrt{s}}{2} \sqrt{1 - 4m_\pi^2/s}$$

and the parameters

$$M_1 = 0.5 \text{ GeV},$$

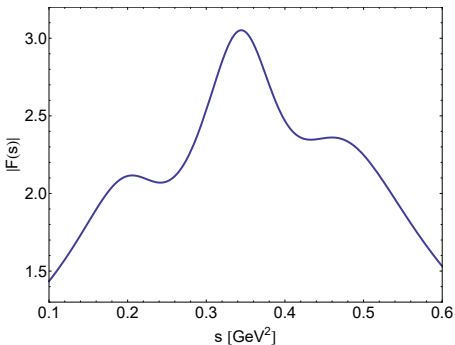
$$\Gamma_1 = 0.2 \text{ GeV},$$

$$M_2 = 0.6 \text{ GeV},$$

$$\Gamma_2 = 0.1 \text{ GeV},$$

$$M_3 = 0.7 \text{ GeV},$$

$$\Gamma_3 = 0.15 \text{ GeV},$$

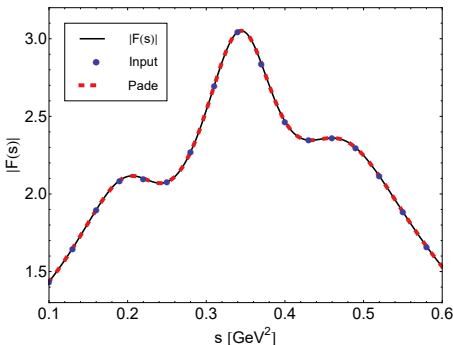


Model for strongly overlapping resonances (II)

$N = 17$ input points were used.

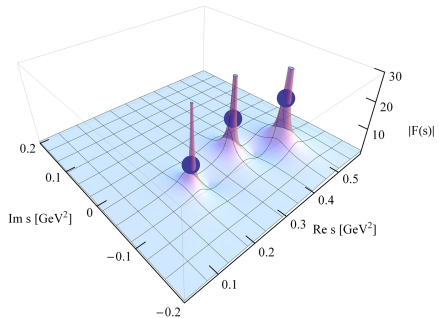
All resonance poles can be reconstructed at the same time since they are in the same analytic regime.

Additional poles can appear in the reconstruction, but they can be easily identified as being unphysical by varying the number of input points or the input region.

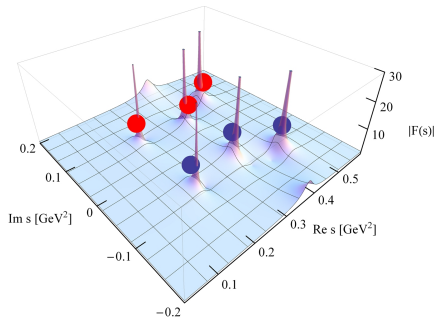


Model for strongly overlapping resonances (III)

exact result, $F(s)$:



reconstruction, $C_M(s)$:

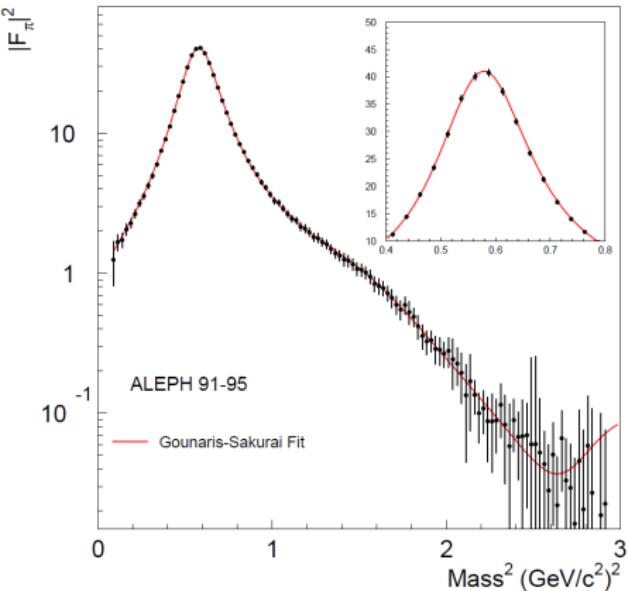


Complex pole of the charged $\rho(770)$ meson

We use the RVP method to analyze the ALEPH data on the squared modulus of the $\pi^-\pi^0$ vector form factor $|F_\pi(s)|^2$.

These data were obtained from τ -lepton decays and represent the cleanest determination of the $\rho(770)$ -meson mass and width.

$$\tau \rightarrow \pi^- \pi^0 \nu_\tau$$



[ALEPH collaboration, Phys. Rept. 421, 191-284, 2005,

arXiv:hep-ex/0506072]

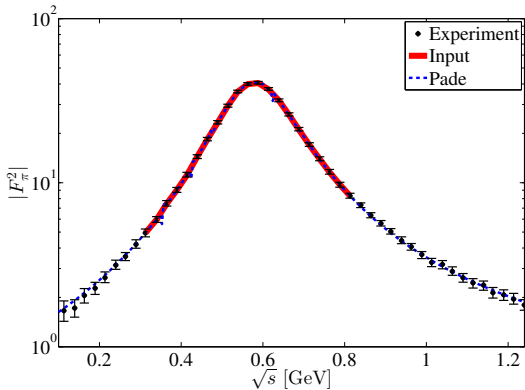
Complex pole of the charged $\rho(770)$ meson

We use the RVP method to analyze the ALEPH data on the squared modulus of the $\pi^-\pi^0$ vector form factor $|F_\pi(s)|^2$.

We find the complex pole of the charged $\rho(770)$ meson to be at $\sqrt{s_\rho} = M_\rho - i\Gamma_\rho/2$ with

$$M_\rho = 761.8 \pm 1.9 \text{ MeV},$$

$$\Gamma_\rho = 139.8 \pm 3.6 \text{ MeV}.$$



[R.-A. T., I. Haritan, J. Wambach and N. Moiseyev, arXiv:1610.03252]

Complex pole of the charged $\rho(770)$ meson

We use the RVP method to analyze the ALEPH data on the squared modulus of the $\pi^-\pi^0$ vector form factor $|F_\pi(s)|^2$.

We find the complex pole of the charged $\rho(770)$ meson to be at $\sqrt{s_\rho} = M_\rho - i\Gamma_\rho/2$ with

$$M_\rho = 761.8 \pm 1.9 \text{ MeV},$$

$$\Gamma_\rho = 139.8 \pm 3.6 \text{ MeV}.$$

M_ρ (MeV)	Γ_ρ (MeV)	source
762.5 ± 2	142 ± 7	[12]
758.3 ± 5.4	145.1 ± 6.3	[13]
$764.1 \pm 2.7^{+4.0}_{-2.5}$	$148.2 \pm 1.9^{+1.7}_{-5.0}$	[14]
754 ± 18	148 ± 20	[15]
763.0 ± 0.2	139.0 ± 0.5	[16]
760 ± 2	147 ± 6	[17]
761 ± 1	139 ± 2	[18]
763.7 ± 1.2	144 ± 3	[19]
761.8 ± 1.9	139.8 ± 3.6	this work

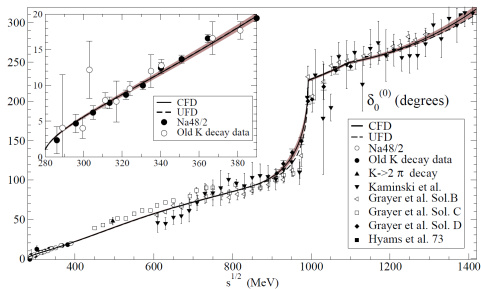
Table 1: Collection of pole parameter predictions for the $\rho(770)$ meson.

[R.-A. T., I. Haritan, J. Wambach and N. Moiseyev, arXiv:1610.03252]

Complex pole of the $f_0(500)$ or σ meson

Locating the resonance pole is particularly difficult for the $f_0(500)$ or σ meson due to its large decay width and the strong overlap with the background and higher resonances.

Plot: S0 wave phase shift for $\pi\pi$ -scattering experimental data together with the UFD and CFD parameterizations.

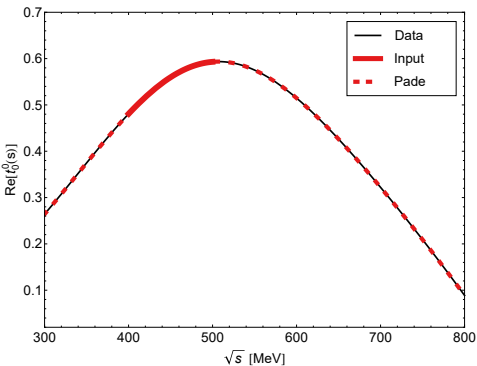


[R. Garcia-Martin, R. Kaminski, J. Pelaez, J. Ruiz de Elvira, and F. Yndurain, Phys.Rev. D83, 074004 (2011), arXiv:1102.2183 [hep-ph]]

Complex pole of the $f_0(500)$ or σ meson

We apply the RVP method to the real part of the S0 partial wave amplitude $t_0^0(s)$ as obtained from the Constrained Fit to Data (CFD) parametrization of the $\delta_0^{(0)}(s)$ phase shift,

$$t_0^0(s) = \frac{\eta_0^0(s)e^{2i\delta_0^0(s)} - 1}{2i\rho_\pi(s)}$$



[R.-A. T., I. Haritan, J. Wambach and N. Moiseyev, arXiv:1610.03252]

We find the complex pole at $\sqrt{s_\sigma} = 450.1 \pm 11.2 - i(299.2 \pm 12.2)$ MeV

Complex pole of the $f_0(500)$ or σ meson

$\sqrt{s_\sigma}$ (MeV)	source
$470 \pm 30 - i(295 \pm 20)$	[24]
$470 \pm 50 - i(285 \pm 25)$	[16]
$441_{-8}^{+16} - i(272_{-12.5}^{+9})$	[25]
$457_{-13}^{+14} - i(279_{-7}^{+11})$	[26]
$442_{-8}^{+5} - i(274_{-5}^{+6})$	[27]
$453 \pm 15 - i(297 \pm 15)$	[28]
$449_{-16}^{+22} - i(275 \pm 12)$	[20]
$450.1 \pm 11.2 - i(299.2 \pm 12.2)$	this work

Table 3: Collection of pole parameter predictions for the $f_0(500)$ or σ meson.

[R.-A. T., I. Haritan, J. Wambach and N. Moiseyev,

arXiv:1610.03252]

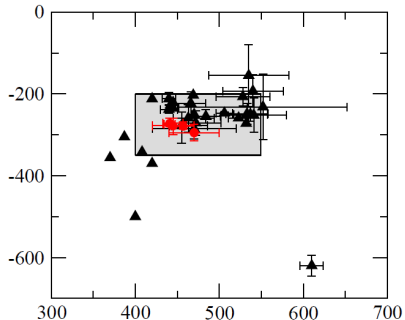


Figure 1: Location of the $f_0(500)$ (or σ) poles in the complex energy plane. Circles denote the recent analyses based on Roy(-like) dispersion relations [8–11], while all other analyses are denoted by triangles. The corresponding references are given in the listing.

[K.A. Olive et al. (Particle Data Group), Chin. Phys. C38, 090001 (2014) (URL: <http://pdg.lbl.gov>)]

Analytic Continuation - Free Particle

We study the spectral function of a free particle:

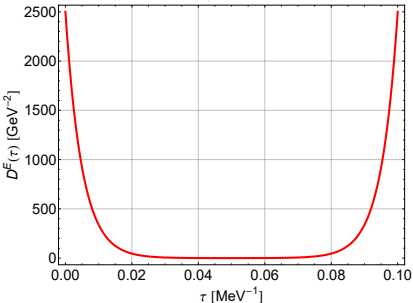
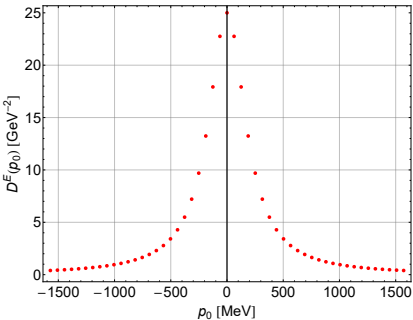
$$\rho(\omega) = \text{sgn}(\omega)\delta(\omega^2 - m^2)$$

The free propagator is given by

$$D^E(p_0) = \frac{1}{p_0^2 + m^2}$$

$$D^E(\tau) = \frac{e^{m(\beta-\tau)} + e^{m\tau}}{2m(e^{m\beta} - 1)}$$

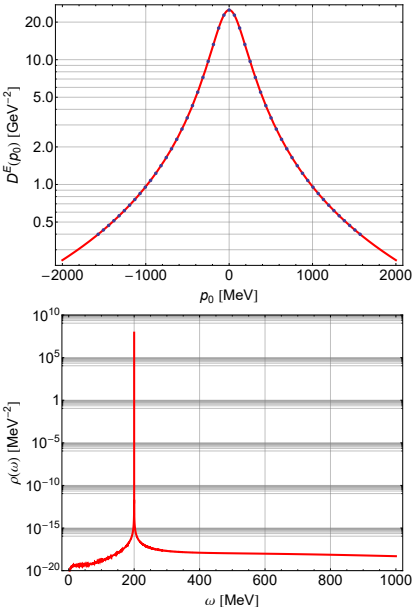
with $p_0 = 2n\pi T$,
 $m = 200$ MeV, and
 $T = 1/\beta = 10$ MeV.



Analytic Continuation - Free Particle

We choose 51 input points from $D^E(p_0)$ and apply the RVP method to obtain $D^R(\omega)$ and the spectral function,

$$\rho(\omega) = -\frac{1}{\pi} \text{Im} D^R(\omega)$$



Analytic Continuation - Breit-Wigner example

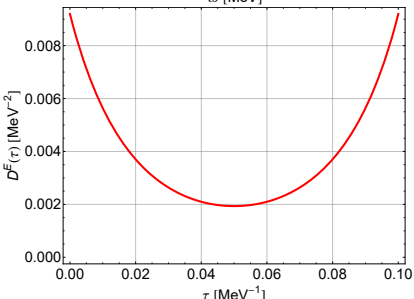
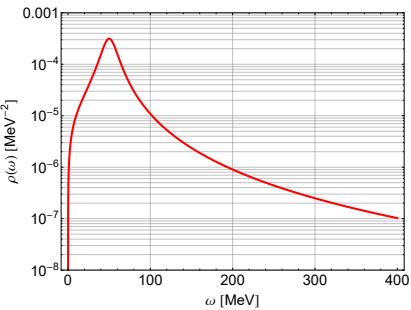
We now study the following Breit-Wigner-type spectral function,

$$\rho(\omega) = \frac{1}{\pi} \frac{2\omega\epsilon}{(\omega^2 - \epsilon^2 - M^2)^2 + 4\omega^2\epsilon^2}$$

We choose $M = 50$ MeV, $\epsilon = 10$ MeV and $T = 1/\beta = 10$ MeV. The propagator is obtained by

$$D^E(\tau) = \int_0^\infty d\omega \rho(\omega) \frac{\cosh(\omega(\tau - \beta/2))}{\sinh(\beta\omega/2)}$$

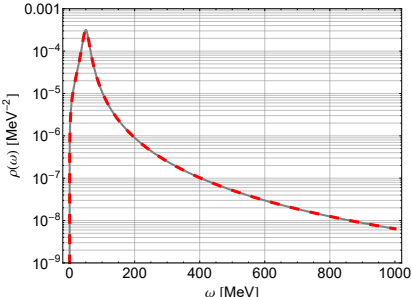
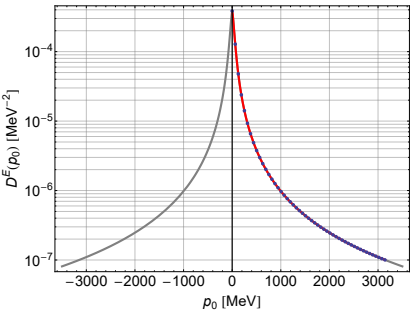
$$D^E(p_0) = \int_{-\infty}^\infty d\omega \frac{\rho(\omega)}{\omega + ip_0}$$



Analytic Continuation - Breit-Wigner example

We choose 51 input points from $D^E(p_0)$ and apply the RVP method to obtain $D^R(\omega)$ and the spectral function,

$$\rho(\omega) = -\frac{1}{\pi} \text{Im} D^R(\omega)$$



Analytic Continuation - More complicated example

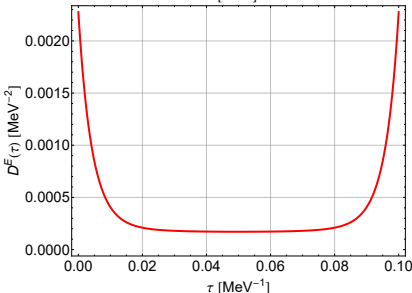
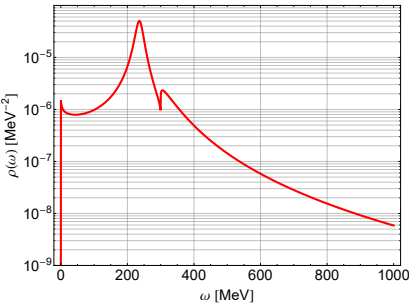
We now study the following spectral function,

$$\rho(\omega) = -\frac{1}{\pi} \text{Im} \left(\frac{1}{(\omega + i\epsilon)^2 - M^2 - \Pi(\omega)} \right)$$

with

$$\begin{aligned}\Pi(\omega) = & S_1 (\ln(T_1^2 - (\omega + i\epsilon)^2)) \\ & + S_2 (\ln(T_2^2 - (\omega + i\epsilon)^2))\end{aligned}$$

We choose $M = 50$ MeV, $\epsilon = 0.1$ MeV, $T = 1/\beta = 10$ MeV, $S_1 = 2000$, $S_2 = 300$, $T_1 = 0$ and $T_2 = 3000$.



Analytic Continuation - More complicated example

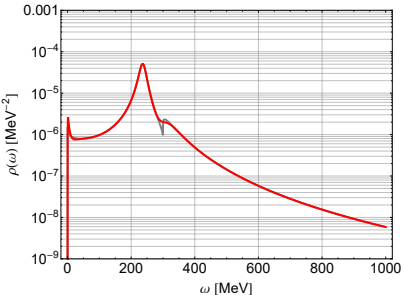
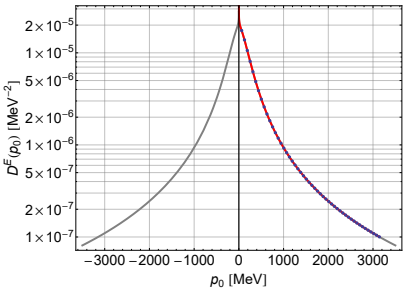
The propagator is obtained by

$$D^E(\tau) = \int_0^\infty d\omega \rho(\omega) \frac{\cosh(\omega(\tau - \beta/2))}{\sinh(\beta\omega/2)}$$

$$D^E(p_0) = \int_{-\infty}^\infty d\omega \frac{\rho(\omega)}{\omega + ip_0}$$

We choose 51 input points from $D^E(p_0)$ and apply the RVP method to obtain $D^R(\omega)$ and the spectral function,

$$\rho(\omega) = -\frac{1}{\pi} \text{Im} D^R(\omega)$$



Analytic continuation - simulating Lattice data

Starting from the spectral function

$$\rho(\omega) = -\frac{1}{\pi} \text{Im} \left(\frac{1}{(\omega + i\epsilon)^2 - M^2 - \Pi(\omega)} \right)$$

we now generate $N = 64$ data points for $D^E(\tau_i)$ by using

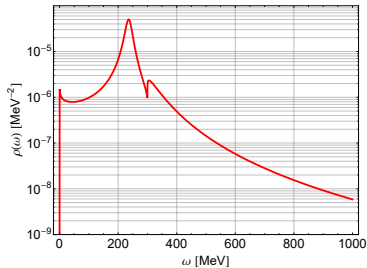
$$D^E(\tau) = \int_0^\infty \frac{\cosh(\omega(\tau - \beta/2))}{\sinh(\beta\omega/2)} \rho(\omega) d\omega$$

Then we apply the discrete Fourier transform to obtain

$$D^E(p_0) = \frac{1}{TN} \sum_{n=-N/2+1}^{N/2} D^E(\tau_n) \exp(ip_0 \tau_n)$$

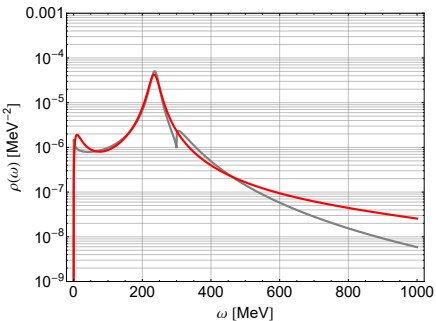
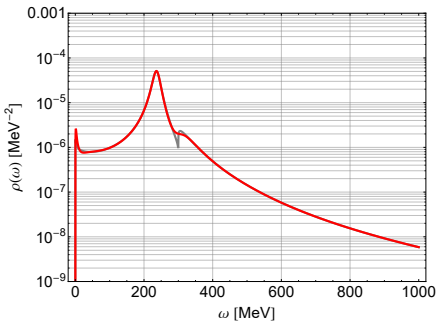
Finally the RVP method is applied to $D^E(p_0)$ to obtain $D^R(\omega)$ the spectral function,

$$\rho(\omega) = -\frac{1}{\pi} \text{Im} D^R(\omega)$$



Analytic continuation - simulating Lattice data

When using a finite number of input points for $D^E(\tau)$ the quality of the input points for $D^E(p_0)$ decreases.

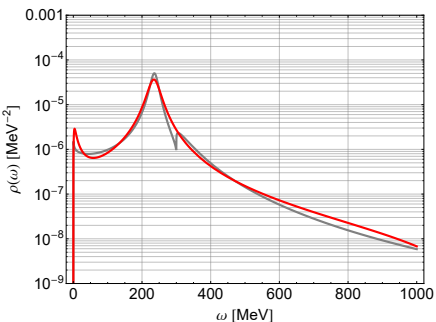


Analytic continuation - simulating Lattice data

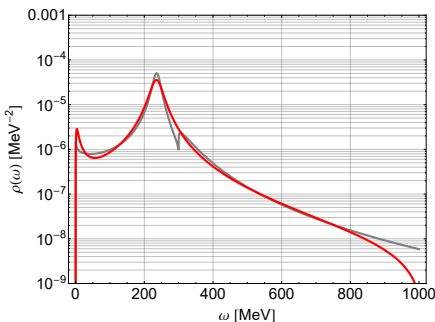
We now add Gaussian noise to the $D^E(\tau_i)$ data ($\mu = D^E(\tau_i)$):

$$f(x) = \frac{1}{\sqrt{2\pi}\sigma} e^{-\frac{(x-\mu)^2}{2\sigma^2}}$$

$$\sigma = \mu/10^6$$



$$\sigma = \mu/10^5$$

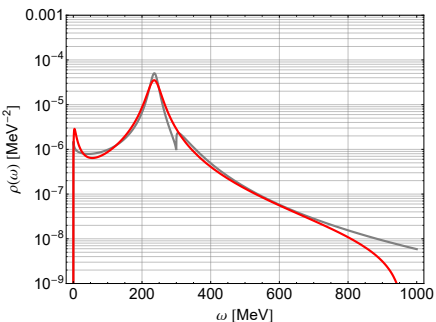


Analytic continuation - simulating Lattice data

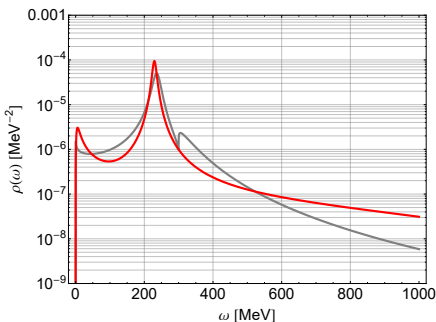
We now add Gaussian noise to the $D^E(\tau_i)$ data ($\mu = D^E(\tau_i)$):

$$f(x) = \frac{1}{\sqrt{2\pi}\sigma} e^{-\frac{(x-\mu)^2}{2\sigma^2}}$$

$$\sigma = \mu/10^4$$



$$\sigma = \mu/10^3$$

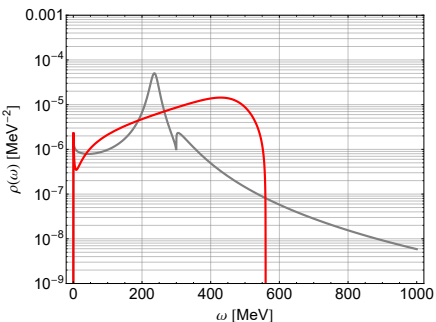


Analytic continuation - simulating Lattice data

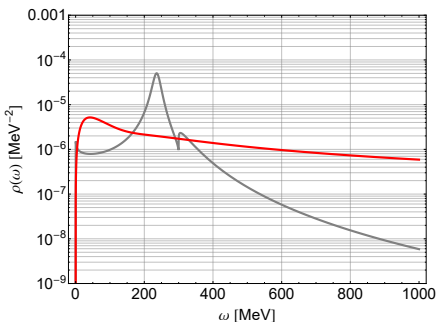
We now add Gaussian noise to the $D^E(\tau_i)$ data ($\mu = D^E(\tau_i)$):

$$f(x) = \frac{1}{\sqrt{2\pi}\sigma} e^{-\frac{(x-\mu)^2}{2\sigma^2}}$$

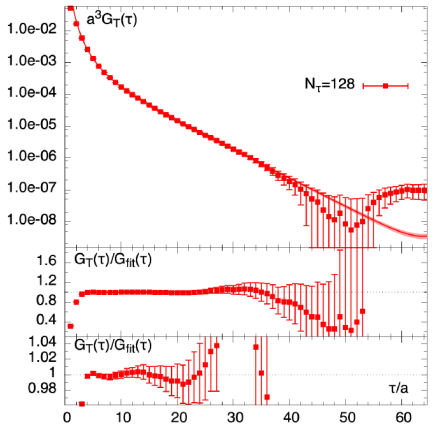
$$\sigma = \mu/10^2$$



$$\sigma = \mu/10^1$$

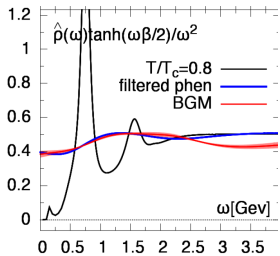


Lattice data on the Rho

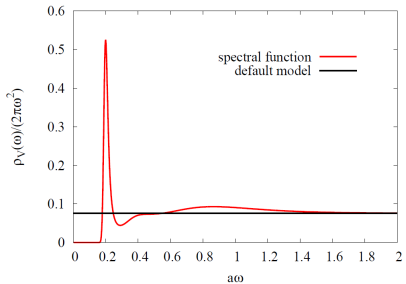


Brandt, Francis, Jäger, Meyer,

arXiv: 1512.07249



Brandt et al.

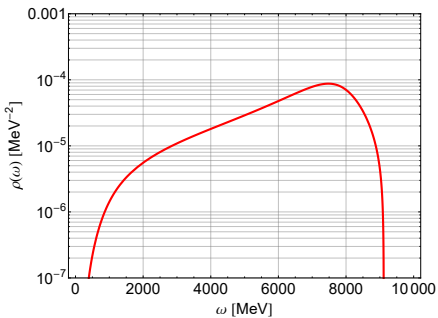
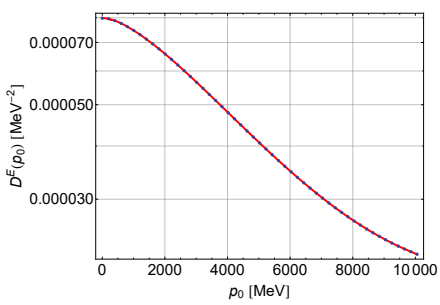


Lattice data on the Rho

We apply the discrete Fourier transform to obtain $N = 50$ points for

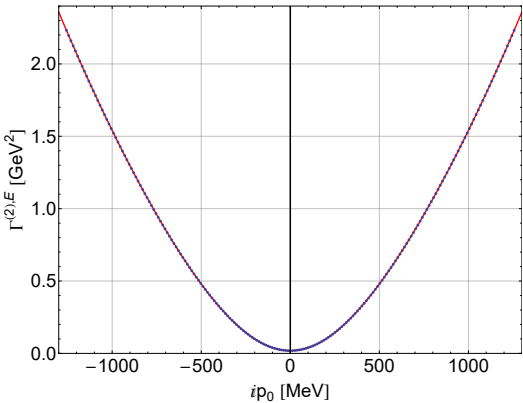
$$D^E(p_0) = \frac{1}{TN} \sum_{n=-N/2+1}^{N/2} D^E(\tau_n) \exp(ip_0\tau_n)$$

Then the RVP method is applied to $D^E(p_0)$ to obtain $D^R(\omega)$ and the spectral function:



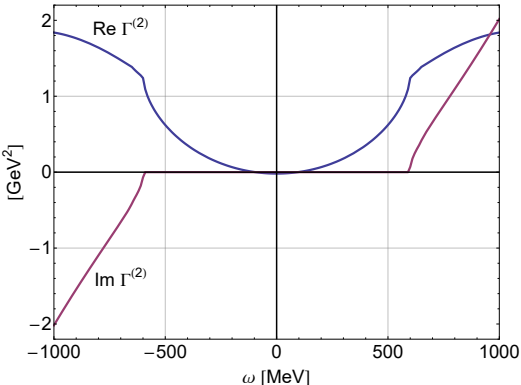
Analytic continuation of Euclidean FRG data

- ▶ We start from data on the Euclidean 2-point function $\Gamma^{(2),E}(ip_0)$ for the pion at $T = 2$ MeV which was obtained using the Functional Renormalization Group approach (FRG)
- ▶ The RVP method is used to obtain the analytic continuation $\Gamma^{(2),R}(\omega)$



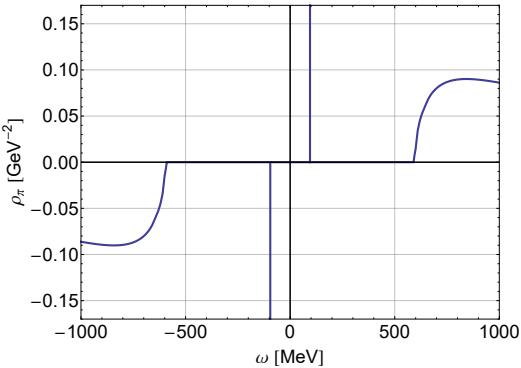
Analytic continuation of Euclidean FRG data

- ▶ the correct result for $\Gamma^{(2),R}(\omega)$ is known and can be used to check the result obtained from the RVP method
- ▶ $\Gamma^{(2),R}(\omega)$ has a non-zero real and imaginary part as well as branch points due to the decay thresholds, in particular at $\omega = 600$ MeV



Analytic continuation of Euclidean FRG data

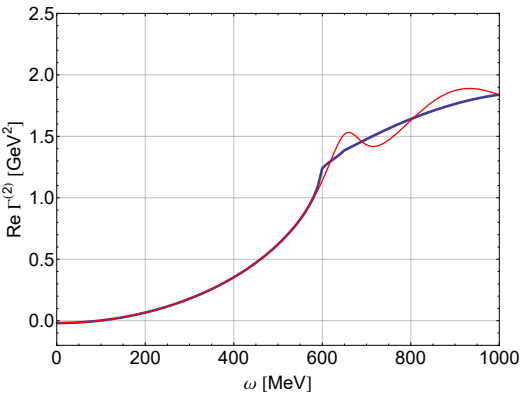
- ▶ the spectral function can be easily obtained from $\Gamma^{(2),R}(\omega)$
- ▶ the branch point at $\omega = 600 \text{ MeV}$ is clearly visible



$$\rho(\omega) = -\frac{1}{\pi} \text{Im} G^R(\omega) = \frac{1}{\pi} \frac{\text{Im} \Gamma^{(2),R}(\omega)}{(\text{Re} \Gamma^{(2),R}(\omega))^2 + (\text{Im} \Gamma^{(2),R}(\omega))^2}$$

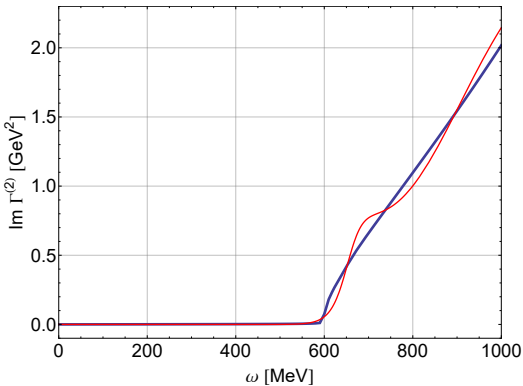
Analytic continuation of Euclidean FRG data

- ▶ $N = 65$ Euclidean input points between $p_0 = 0$ MeV and $p_0 = 2000$ MeV are used
- ▶ we can reproduce the low-energy part of $\Gamma^{(2),R}(\omega)$ and also get a good estimate for energies beyond the branch point at $\omega = 600$ MeV



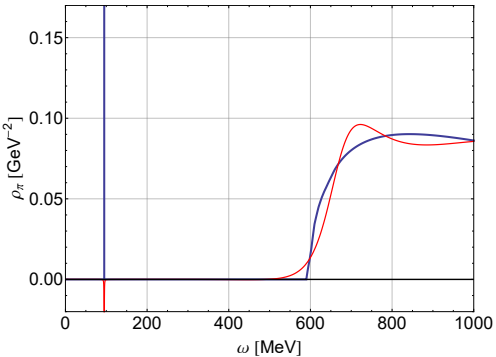
Analytic continuation of Euclidean FRG data

- ▶ $N = 65$ Euclidean input points between $p_0 = 0$ MeV and $p_0 = 2000$ MeV are used
- ▶ we can reproduce the low-energy part of $\Gamma^{(2),R}(\omega)$ and also get a good estimate for energies beyond the branch point at $\omega = 600$ MeV



Analytic continuation of Euclidean FRG data

- ▶ $N = 65$ Euclidean input points between $p_0 = 0$ MeV and $p_0 = 2000$ MeV are used
- ▶ we can reproduce the low-energy part of $\Gamma^{(2),R}(\omega)$ and also get a good estimate for energies beyond the branch point at $\omega = 600$ MeV



Summary

The Resonances Via Padé (RVP) method can be used to obtain the analytic continuation of a function that is given in numerical form.

- ▶ only requires real input in order to reconstruct the underlying function not only along the real axis but also in the complex plane
- ▶ can be used to identify resonance poles and to predict decay thresholds
- ▶ can in principle be used to obtain real-time information starting from Euclidean data with small errors